ELSEVIER

Journal of Alloys and Compounds 446–447 (2007) 121–123

Journal of ALLOYS AND COMPOUNDS

www.elsevier.com/locate/jallcom

The hydrogen desorption kinetics of $Mg_{0.9-x}Ti_{0.1}Pd_xNi$ ($x = 0.04, 0.06, 0.08, 0.1$) electrode alloys

Qi-Feng Tian [a,b], Yao Zhang [a,*], Li-Xian Sun [a,*], Fen Xu [a], Hua-Tang Yuan [c]

[a] *Dalian Institute of Chemical Physics, Chinese Academy of Sciences, Dalian 116023, China*
[b] *Hubei Key Laboratory of Novel Chemical Reactor & Green Chemical Technology, Wuhan Institute of Technology, Wuhan 430073, China*
[c] *Institute of New Energy Material Chemistry, Nankai University, Tianjin 300071, China*

Received 13 September 2006; received in revised form 23 December 2006; accepted 5 January 2007
Available online 11 January 2007

Abstract

We have reported that the cyclic stability of $Mg_{0.9-x}Ti_{0.1}Pd_xNi$ ($x = 0.04, 0.06, 0.08, 0.1$) amorphous electrode alloys prepared by mechanical alloying was enhanced to 100 cycles over 200 mAh/g in our previous work. The hydrogen desorption kinetics of the electrode alloys were studied in this work by potentiostatic discharge experiments. Experimental results showed that the three-dimensional hydrogen diffusion dominated the desorption process of electrode alloys. The activation energy of desorption was calculated according to the Arrenius equation. The values were 49.11 kJ mol^{-1}, 45.99 kJ mol^{-1}, 42.50 kJ mol^{-1} and 40.66 kJ mol^{-1} for $x = 0.04$, 0.06, 0.08 and 0.1 of $Mg_{0.9-x}Ti_{0.1}Pd_xNi$ electrode alloys, respectively. The limiting current densities were determined by anodic polarization experiments. The increasing Pd amount results in the reducing of activation energy and enhancement of the limiting current density of the quaternary Mg-based electrode alloys.

Keywords: Hydrogen desorption kinetics; Potentiostatic discharge; Three-dimensional diffusion; Activation energy; Hydrogen storage alloys

1. Introduction

Mg-based alloy is potential candidate for cathode materials of Ni-MH rechargeable batteries due to its large discharge capacity and low cost [1]. However, its poor cyclic stability cannot meet the need of application. Many efforts of element substitutions in the alloy have been tried to improve its cyclic performances [2–4]. The doped Ti or Pd in the Mg–Ni-based alloys exhibited significant effects [5–9]. In our previous work, $Mg_{0.9-x}Ti_{0.1}Pd_xNi$ ($x = 0.04, 0.06, 0.08, 0.1$) quaternary alloys were synthesized and its structure were determined as amorphous by X-ray diffraction (XRD) and selected area electron diffraction (SAED) of transmission electron microscopy (TEM) [10]. We found that the synergetic substitution of Pd and Ti for Mg in Mg–Ni ternary electrode alloy showed high cyclic stability (100 cycles over 200 mAh/g).

Besides cyclic dischargeability, the reaction kinetics is also crucial for hydrogen storage alloy electrode. Northwood and co-workers [11] ever studied the hydrogen desorption (discharge) kinetics of $LaNi_{4.7}Al_{0.3}$ electrode alloy by means of potentiostatic measurements. They found that phase transformation ($\beta \rightarrow \alpha$) controlled the hydrogen desorption process of $LaNi_{4.7}Al_{0.3}$ electrode within the temperature range from 289 K to 328 K and the applied potential range from −0.80 V to −0.60 V (versus Hg/HgO electrode). This idea is also available in the hydrogen desorption kinetics of Mg-based hydrogen storage electrode alloy. In the present work, the discharge kinetics of $Mg_{0.9-x}Ti_{0.1}Pd_xNi$ ($x = 0.04, 0.06, 0.08, 0.1$) electrode alloys was investigated by means of potentiostatic discharge technique. The anodic polarization tests were used to verify the kinetic results obtained from potentiostatic discharge measurements.

2. Experimental

$Mg_{0.9-x}Ti_{0.1}Pd_xNi$ ($x = 0.04, 0.06, 0.08, 0.1$) alloys were prepared by mechanical alloying (MA). The purity of all metallic powders was higher than 99.5%. The metallic powders with designed stoichiometry were ground in a planetary mill with a ball to powder weight ratio of 30:1 under Ar atmosphere for 120 h.

The working electrode materials to be tested were the pressed mixture of 0.1 g alloy powder with 0.3 g electrolytic Cu powder. The $NiOOH/Ni(OH)_2$ electrode and Hg/HgO electrode were used as counter and reference electrode, respec-

* Corresponding authors. Tel.: +86 411 84379215; fax: +86 411 84685940.
E-mail addresses: zhangyao@dicp.ac.cn (Y. Zhang), lxsun@dicp.ac.cn (L.-X. Sun).

0925-8388/$ – see front matter © 2007 Elsevier B.V. All rights reserved.
doi:10.1016/j.jallcom.2007.01.004

tively. The electrolyte was 6 M KOH aqueous solution. The electrodes were charged for 3 h at a current density of 300 mA/g and then discharged at a current density of 100 mA/g until 50% depth of discharge (DOD). The potentiostatic discharge and anodic polarization measurements were conducted on Zahner Elektrik IM6e electrochemical workstation. The potentiostatic discharge tests were executed at the end of charge and the applied potential was −0.7 V (versus Hg/HgO electrode). The discharge temperatures were 298 K, 303 K and 313 K, respectively. The discharge experiments were terminated when the discharge current was less than 1 mA. The anodic polarization curves were measured from 0 mV to 500 mV (versus open circuit potential) with a scanning rate of 1 mV/s at 50% DOD and 303 K.

3. Results and discussion

3.1. Potentiostatic discharge

For potentiostatic discharge tests the integration of $I(t)$ versus time curve represent as total charge. Thus, the reacted fraction $\alpha(t)$ during the discharge can be defined as follows:

$$\alpha(t) = \frac{\int_0^t I(t)\,\mathrm{d}t}{\int_0^\infty I(t)\,\mathrm{d}t} \quad (1)$$

where $\int_0^\infty I(t)\,\mathrm{d}t$ is the maximum charge during the discharge process and $\int_0^t I(t)\,\mathrm{d}t$ is the charge at the time of t. Usually, the desorption kinetics can be analyzed by fitting the experimental curves with the rate equations which derived from different processes. Considering the amorphous structures of the studied alloys, several possible kinetics equations were used to fit the experimental data [12]. Table 1 summarizes the used kinetics equations and related hydrogen desorption mechanisms. In the present work, the hydrogen desorption curves of $Mg_{0.9-x}Ti_{0.1}Pd_xNi$ ($x = 0.04$, 0.06, 0.08, 0.1) electrode alloys can be fitted with good accuracy by Jander diffusion model,

Table 1
Mechanisms and the kinetics equations used to fit the experimental data

Mechanism	Kinetics equation	r
Chemical reaction	$1-(1-\alpha)^r = kt$	1/2, 2, 3, 4, 1/4, 1/3
	$(1-\alpha)^{-2} = kt$	
	$(1-\alpha)^{-1} - 1 = kt$	
	$(1-\alpha)^{-1} = kt$	
	$(1-\alpha)^{-1/2} = kt$	
1-Dimensional diffusion	$\alpha^2 = kt$	
2-Dimensional diffusion	$\alpha + (1-\alpha)\ln(1-\alpha) = kt$	
	$[1-(1-\alpha)^{1/2}]^2 = kt$	
	$[1-(1-\alpha)^{1/2}]^{1/2} = kt$	
3-Dimensional diffusion	$[1-(1-\alpha)^{1/3}]^2 = kt$	
	$[1-(1-\alpha)^{1/3}]^{1/2} = kt$	
	$1 - 2\alpha/3 - (1-\alpha)^{2/3} = kt$	
	$[(1+\alpha)^{1/3} - 1]^2 = kt$	
	$[(1-\alpha)^{(-1/3)} - 1]^2 = kt$	
	$(1+\alpha)^{2/3} + (1-\alpha)^{2/3} = kt$	

α denotes as reacted fraction; k and t represent rate constant and time, respectively.

whose kinetics equation is

$$[1-(1-\alpha)^{1/3}]^2 = kt \quad (2)$$

where α is the reacted fraction, k and t represent rate constant and time, respectively.

The relationships between $[1-(1-\alpha(t))^{1/3}]^2$ and t for $Mg_{0.9-x}Ti_{0.1}Pd_xNi$ ($x = 0.04$, 0.06, 0.08, 0.1) electrode alloys are plotted in Fig. 1. The straight lines in the figure are the fitted lines using the Eq. (2) and experimental data are the discrete dots. The plots are not linear over the entire reaction range, since a deviation from the fitted line was found at the initial

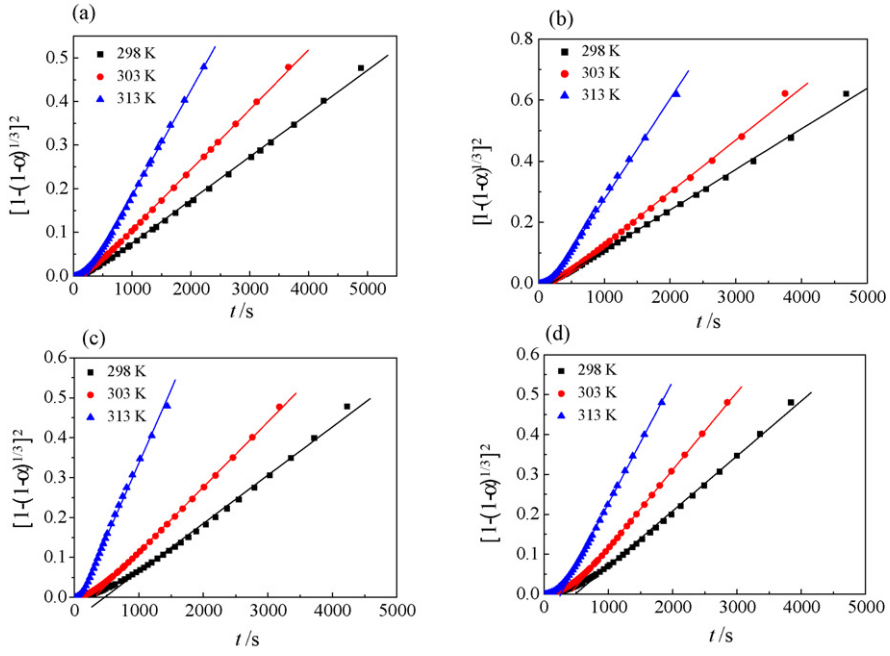

Fig. 1. The relationship between $[1-(1-\alpha(t))^{1/3}]^2$ and t at various temperatures for $Mg_{0.9-x}Ti_{0.1}Pd_xNi$ ($x = 0.04$, 0.06, 0.08, 0.1) electrode alloys. (a) $Mg_{0.86}Ti_{0.1}Pd_{0.04}Ni$; (b) $Mg_{0.84}Ti_{0.1}Pd_{0.06}Ni$; (c) $Mg_{0.82}Ti_{0.1}Pd_{0.08}Ni$; (d) $Mg_{0.8}Ti_{0.1}Pd_{0.1}Ni$.

Table 2
The relationship between activation energy of hydrogen desorption and the limiting current densities of $Mg_{0.9-x}Ti_{0.1}Pd_xNi$ ($x = 0.04, 0.06, 0.08, 0.1$) electrode alloys

x	Activation energy (kJ mol^{-1})	Limiting current density (mA g^{-1})
0.04	49.11	916
0.06	45.99	1063
0.08	42.50	1096
0.10	40.66	1129

stage of discharge. Such deviation was resulted from the surface charge transfer instead of three-dimensional diffusion being the rate control step at the initial stage of discharge. However, the hydrogen diffusion dominated the majority of the discharge process for the studied alloys, which was verified with the fact that the fitted lines were close to most of the experimental data points in the figure. Similar results were obtained for the amorphous $LaNi_5$ type films [13], which was concluded that the hydrogen desorption was controlled by the hydrogen diffusion in the amorphous La–Ni films. The disordered structures of amorphous alloys do not possess certain channels such as grain boundaries or interfaces for rapid hydrogen diffusion [14], which resulted in the slow reaction kinetics and the hydrogen diffusion dominated the hydrogen desorption in this work.

It was found that the relationship between the $\ln k$ and $1/T$ for $Mg_{0.9-x}Ti_{0.1}Pd_xNi$ ($x = 0.04, 0.06, 0.08, 0.1$) electrode alloys is linear, which indicated that the relationship between these two parameters is Arrhenius equation. The desorption activation energies can be calculated and its results are listed in Table 2. From the table we can see that the activation energies of electrode alloys decreased with the increase of Pd content, which means the hydrogen desorption capacities of the electrode alloys strengthened with the increase of Pd content.

3.2. Anodic polarization

The polarization curves of $Mg_{0.9-x}Ti_{0.1}Pd_xNi$ ($x = 0.04, 0.06, 0.08, 0.1$) electrode alloys measured at 50% DOD and 303 K. It is well known that the limiting current density can be determined from the curve, and its value denotes the hydrogen diffusion capacities of the electrode alloys. The limiting current densities of the electrode alloys are also summarized in Table 2. It can be seen that its value increased from 916 mA/g ($x = 0.04$) to 1129 mA/g ($x = 0.1$). With the increase of Pd, the tendency of limiting current density is consistent with the activation energy of hydrogen desorption, which were obtained from potentiostatic discharge experiments.

4. Conclusions

The hydrogen desorption is mainly dominated by three-dimensional hydrogen diffusion for $Mg_{0.9-x}Ti_{0.1}Pd_xNi$ ($x = 0.04, 0.06, 0.08, 0.1$) electrode alloys. The increasing Pd amount reduces the activation energy but improves the limiting current density of the quaternary Mg-based electrode alloys.

Acknowledgement

This work was supported by the National Natural Science Foundation of China, Grant No. 20473091.

References

[1] Y.Q. Lei, Y.M. Wu, Q.M. Yang, J. Wu, Q.D. Wang, Z. Phys. Chem. Bd. 183 (1994) 379–384.
[2] S. Nohara, K. Hamasaki, S.G. Zhang, H. Inoue, C. Iwakura, J. Alloys Compd. 280 (1998) 104–106.
[3] W.H. Liu, H.Q. Wu, Y.Q. Lei, Q.D. Wang, J. Wu, J. Alloys Compd. 261 (1997) 289–294.
[4] H. Ye, Y.Q. Lei, L.S. Chen, H. Zhang, J. Alloys Compd. 311 (2000) 194–199.
[5] S.-C. Han, P.S. Lee, J.-Y. Lee, A. Züttel, L. Schlapbach, J. Alloys Compd. 306 (2000) 219–226.
[6] Y. Zhang, S.-K. Zhang, L.-X. Chen, Y.-Q. Lei, Q.-D. Wang, Int. J. Hydrogen Energy 26 (2001) 801–806.
[7] S. Ruggeri, L. Roué, J. Huot, R. Schulz, L. Aymard, J.-M. Tarascon, J. Power Sources 112 (2002) 547–556.
[8] T. Ma, Y. Hatano, T. Abe, K. Watanabe, J. Alloys Compd. 372 (2004) 251–258.
[9] T. Ma, Y. Hatano, T. Abe, K. Watanabe, J. Alloys Compd. 391 (2005) 313–317.
[10] Q.-F. Tian, Y. Zhang, L.-X. Sun, F. Xu, Z.-C. Tan, H.-T. Yuan, T. Zhang, J. Power Sources 158 (2006) 1463–1471.
[11] F. Feng, J.W. Han, M.M. Geng, D.O. Northwood, Solar Energy Mater. Solar Cells 62 (2000) 51–61.
[12] Q. Li, Q. Lin, K.-C. Chou, L.-J. Jiang, J. Mater. Sci. 39 (2004) 61–65.
[13] F. Cuevas, M. Hirscher, J. Alloys Compd. 313 (2000) 269–275.
[14] M. Au, Mater. Sci. Eng. B 117 (2005) 37–44.